IOP Publishing Journal of Physics D: Applied Physics
J. Phys. D: Appl. Phys. **51** (2018) 123001 (12pp) https://doi.org/10.1088/1361-6463/aaac6d

Topical Review

Review of status developments of high-efficiency crystalline silicon solar cells

Jingjing Liu, Yao Yao, Shaoqing Xiao and Xiaofeng Gu

Department of Electronic Engineering, Engineering Research Center of IOT Technology Applications (Ministry of Education), Jiangnan University, Wuxi 214122, People's Republic of China

E-mail: larring0078@hotmail.com

Received 11 November 2017, revised 16 January 2018
Accepted for publication 1 February 2018
Published 20 February 2018

Abstract

In order to further improve cell efficiency and reduce cost in achieving grid parity, a large number of PV manufacturing companies, universities and research institutes have been devoted to a variety of low-cost and high-efficiency crystalline Si solar cells. In this article, the cell structures, characteristics and efficiency progresses of several types of high-efficiency crystalline Si solar cells that have been in small scale production or are promising in mass production are presented, including passivated emitter rear cell, tunnel oxide passivated contact solar cell, interdigitated back contact cell, heterojunction with intrinsic thin-layer cell, and heterojunction solar cells with interdigitated back contacts. Both the industrialization status and future development trend of high-efficiency crystalline silicon solar cells are also pinpointed.

Keywords: high efficiency crystalline silicon solar cells, PERC, IBC, HIT, HBC

(Some figures may appear in colour only in the online journal)

1. Introduction

Since the first real silicon p-n junction solar cell in the world was successfully developed in Bell Labs [1], silicon solar cells have always been on a steady uptrend. In the early stage, the cell efficiency was improved mainly due to classical semiconductor technology such as diffusion. In the 1990s and 2000s, novel technologies such as surface texturing, screen printing, passivated emitter and rear contact, and firing technology were introduced, and these technologies played a key role in improving the cell efficiency and reducing the production cost and thus promoted the industrialization of Si photovoltaics (PV). Up to now, crystalline silicon solar cells including polycrystalline and monocrystalline technologies are the most important photovoltaic technology with a global photovoltaic market share of about 90%. At present, polycrystalline and monocrystalline silicon solar cells with traditional aluminum back surface field process have achieved efficiency of 19.8% and 18.5%, respectively [2–5], very close to the limit of the current crystalline silicon production line. In order to further enhance the cell efficiency and reduce the cost and then achieve the goal of PV grid parity, the major PV companies such as Solar World, Trina Solar, JinKo Solar, Canadian Solar Inc., Hebei JA Solar, GCL Solar Energy, Wuxi Suntech, and Zhejiang Astronergy have turned to research and development of a variety of high-efficiency, low-cost crystalline silicon solar cells [6–13].

Therefore, Si solar cell conversion efficiency has been refreshed time and time again due to the improvements in high-efficiency technologies. In 2014, Panasonic, Sharp and SunPower reported the efficiencies of 25.6% [14], 25.1% [15] and 25.0% [16], respectively, all of which broke the historical record set by the University of New South Wales (UNSW) in 1999 [17]. Until now, the world record efficiency has been raised to 26.6% by Kaneka, Japan [18]. Accelerating technological progress to improve conversion efficiency is the key to reduce the cost of photovoltaic generation.

Crystalline silicon solar cells generate PV power including the following physical processes: (i) photon absorption leading to excitation of electron–hole pairs and (ii) separation and transport of electron–hole pairs to external electrodes [19–24]. Therefore, high efficiency crystalline silicon solar cell technology usually involves the design of a novel cell structure, the optimization of light absorption, the effective collection of photo-generated carriers, the suppression of photo-generated carriers recombination loss as well as the electrode resistance and the area reduction. These technologies produce a series of high efficiency crystalline silicon solar cells, such as passivated emitter rear cell (PERC), interdigitated back contact cell (IBC), heterojunction with intrinsic thin-layer cell (HIT), and heterojunction solar cells with interdigitated back contacts (HBC). According to the latest International Technology Roadmap for Photovoltaic (eighth edition, ITRPV) 2017 [25], back surface field (BSF) cells will still dominate the market in the next few years, but PERC/PERL/PERT, HIT and IBC cells will gain significant market share over back surface field (BSF) cells, and HIT and IBC cells will become more important. In 2014, we have reviewed materials, devices, physics, development and status of high-efficiency Si solar cells developed over the last 20 years [26, 27]. Nevertheless, high-efficiency Si solar cells developed surprisingly fast and many advanced technologies with superior performances were achieved especially in the past three years. This motivated us to write this review article, which aims to present the progress of high-efficiency Si solar cells achieved in the past three years. We carefully discuss device structure and physics mechanism of various high efficiency Si solar cells that are being in rapid development in the past three years. In addition, the latest progress of each high efficiency crystalline silicon solar cells is reviewed and the corresponding potential and challenge for large-scale commercial application is also pinpointed.

2. High-efficiency crystalline silicon solar cells

2.1. PERC solar cell

In early 1983, the concept of passivated emitter rear cell [28] was first proposed by Martin Green at the University of New South Wales, Australia. A record efficiency of 22.8% was obtained by Blakers *et al* for small-area PERC solar cells based on p-type FZ Si substrates in 1989 [29]. Compared to conventional solar cells, the efficiency improvement is mainly due to its structural and technological improvements.

PERC solar cell means to add a rear passivation scheme to the standard full-area Al-BSF cell, concretely involving the deposition of a rear surface passivation film, which is subsequently and locally opened to give way for the formation of a rear contact, as shown in figure 1. The optimization of the rear surface aiming at reducing recombination losses on the cell's back side gets rid of the inherent limitations of the metallic film of aluminum in BSF solar cells, so the electrical and optical losses are reduced. In addition, the optimization of the rear side is fully independent from the front side, which means that further optimization on the front side, such as employing innovative metallization concepts and improved junction properties, can further improve cell performance for PERC structure. PERC solar cell is highly compatible with the existing PV production lines and thus is one of the simplest technologies among all kinds of high-efficiency crystalline silicon solar cell technologies. As a result, a small increase in production cost is required, making it preferred for many crystalline silicon solar cell manufacturers.

The key point of PERC cell is the deposition of the rear passivation film. In general, passivation layer stacks such as Al_2O_3/SiN_x or SiO_2/SiN_x are applied as the rear side passivation scheme for high-efficiency PERC cells [30]. On one hand, by saturating the dangling bonds on the silicon rear surface, Al_2O_3 shows outstanding chemical passivation; on the other hand, high fixed negative charge density($\sim Q_{fix} = 10^{13}$ cm^{-2}) enable Al_2O_3 as an excellent field effect passivation scheme [31]. The Al_2O_3 layer capped by a following deposited SiN_x layer can further enhance the passivation effect because SiN_x layer protects the rear passivation film from metallization. In addition, since Al_2O_3 is typically thin, SiN_x layer can compensate for the rear passivation stack thickness to ensure enough internal reflection on the back of the cell and thus enhance the long wave response and improve the short-circuit current. The seventh edition ITRPV 2016 predicts that Al_2O_3 will gain more PERC market share from 97% at present to 100% in 2020 [25]. In general, Al_2O_3 can be deposited by atomic layer deposition (ALD) [32–34] or plasma enhanced chemical vapor deposition (PECVD) [35–43]. After the deposition of rear passivation stack, lase contact opening is often used to locally ablate the dielectric passivation layer for contact formation between Al and silicon.

The Ag paste consumption increases with the development of PV industry year by year, and therefore, the price of Ag paste increases limiting the harmonious development of low cost and high throughput in solar cell industry. As a result, reducing the Ag paste consumption develops into one of the most important goals. In 2014, Institute for solar energy research hamelin (ISFH) applied a 5-busbar front grid and fine line-printed Ag fingers to industrial-type PERC solar cells and achieved an average conversion efficiency of 21.2%, which is in stark contrast to an average conversion efficiency of 20.6% efficiency for the 3-busbar PERC solar cell [44]. This improved conversion efficiency is primarily due to an increased short circuit current resulting from the reduced shadowing loss, secondly to an increased open-circuit voltage caused by the reduced metal contact area, and finally to an increased fill factor (FF) originating from the reduced resistance losses of the finger grid. At the same time, lower Ag paste consumption was required for such multi-busbar PERC solar cell in comparison with the 3-busbar PERC solar cell, significantly reducing the production cost. Nevertheless, such multi-busbar PERC technology may have a higher demand for module interconnection technology.

ISFH also systematically studied two emitter formation technologies on industrial PERC solar cells including *in situ* oxidation and gas phase etch back (GEB) [45], which can reduce the phosphorus surface concentration to 7×10^{19} cm^{-3} and 4×10^{19} cm^{-3}, respectively, thereby significantly decreasing Shockley–Read–Hall and Auger recombination.

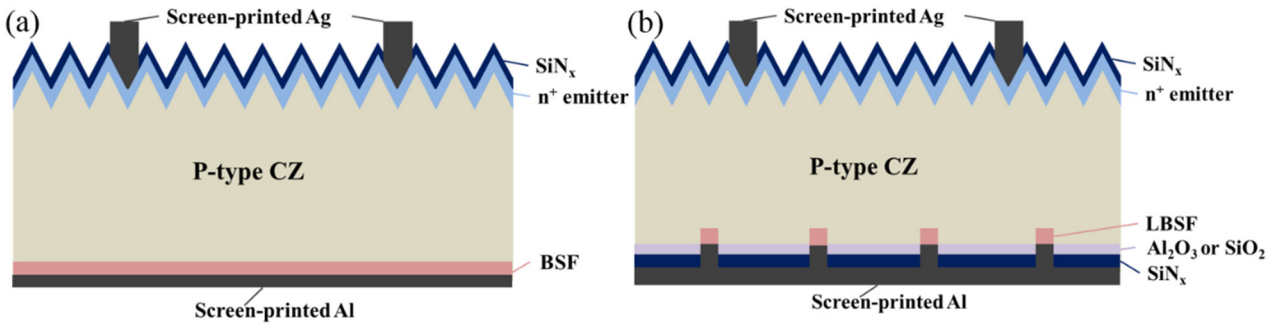

Figure 1. Schemes of (a) standard full-area Al-BSF cell and (b) PERC solar cell with screen-printed front and rear contacts with Al_2O_3/SiN_x or SiO_2/SiN_x rear passivation stacks. LBSF represents the local back surface field.

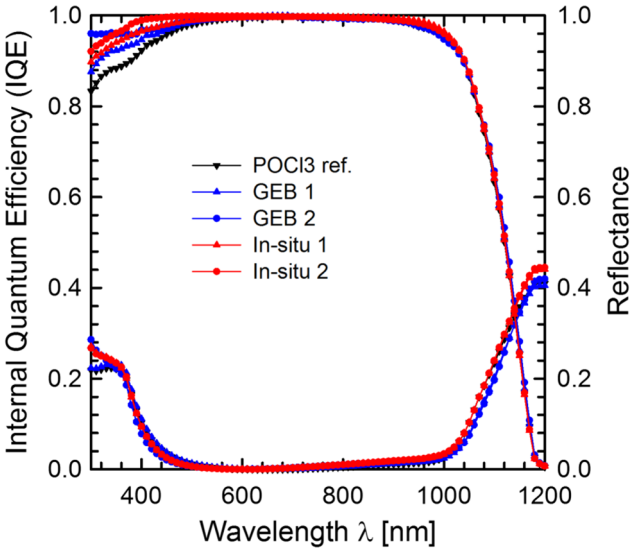

Figure 2. Internal quantum efficiency (IQE) and reflectance measurements of the PERC solar cells with different emitter technologies. [45] John Wiley & Sons. Copyright © 2016 John Wiley & Sons, Ltd.

Accordingly, the emitter saturation current density was reduced to 22 fA cm^{-2} and 28 fA cm^{-2} for *in situ* oxidation and GEB, respectively, with similar emitter sheet resistances of around 150 Ω/sq. Figure 2 shows the internal quantum efficiency (IQE) and reflectance measurements of PERC solar cells with different emitter technologies. In the blue wavelength range between 300 nm and 500 nm, the *in situ* and GEB emitters clearly exhibit a higher IQE value than the conventional $POCl_3$ diffusion, demonstrating the reduced emitter recombination because of the reduced front surface phosphorus concentration. Therefore, conversion efficiency of approaching 22% was achieved.

In July 2015, German manufacturer SolarWorld achieved an efficiency of 21.7% for PERC cells, whereas Trina Solar in China, a global leader in PV modules, breaking the PERC efficiency record for many times in recent years, realized an efficiency of 22.13% in December of the same year [46]. In January 2016, SolarWorld achieved a production line conversion efficiency of 22.04% using selective emitter technology [47]. Later in December, Trina Solar announced a new world conversion efficiency record of 22.61% for advanced PERC cells using a low-cost industrial process that integrates back surface passivation, front surface advanced passivation

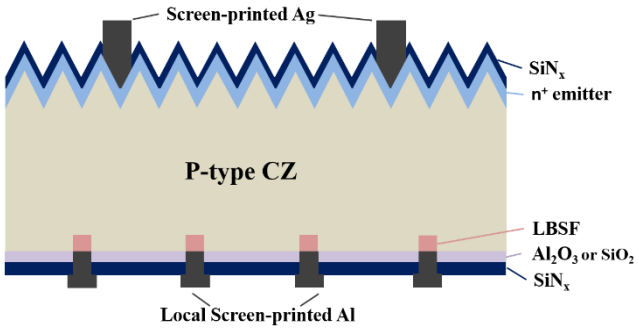

Figure 3. Scheme of a bifacial PERC solar cell with rear Al finger grid. The use of screen-printed rear Al finger grid instead of the conventional full-area Al rear metallization can drastically reduce the Al paste consumption.

and anti-LID (light induced degradation) technologies on a large-sized (243.23 cm^2) boron-doped CZ-Si substrate [48]. Recently in November 2017, LERRI Solar reached a record conversion efficiency of 23.26%, breaking its previous record efficiencies of 22.71%, 22.43% and 22.17% set in the same year. Naturally, LERRI Solar maintained its global leadership position in the PERC cell industry [49].

For polysilicon PERC cells, Trina Solar set an efficiency record of 21.25% on a large area (156 mm × 156 mm) p-type mc-Si substrate in 2016 [50]. But soon the record was broken by JinkoSolar who achieved a conversion efficiency of up to 21.63% [51]. The reason for such high efficiency is mainly due to excellent light absorption and very low surface recombination velocity resulting from advanced light trapping, passivation and hydrogenation technology as well as the high quality of the polysilicon material with a bulk lifetime exceeding 500 μs. In 2017, the efficiency of polysilicon PERC solar cells was further promoted by JinkoSolar to 22.04% [52], which is the first time exceeding 22% for polysilicon PERC solar cells.

Additionally, bifacial PERC cell, namely the PERC+ cell [53, 54] developed by ISFH is a novel, simple and economical design, and does not need any additional steps apart from the typical PERC processing. The emergence of bifacial PERC cells enhance the competitiveness of PERC cells again. The scheme of such bifacial PERC cell is shown in figure 3. The use of screen-printed rear Al finger grid instead of the conventional full-area aluminum rear metallization, in combination with the 5-busbar layout, the Al paste consumption of the PERC+ cells is drastically reduced to 0.15 g, which compares to 1.6 g for the conventional PERC cells with full-area Al

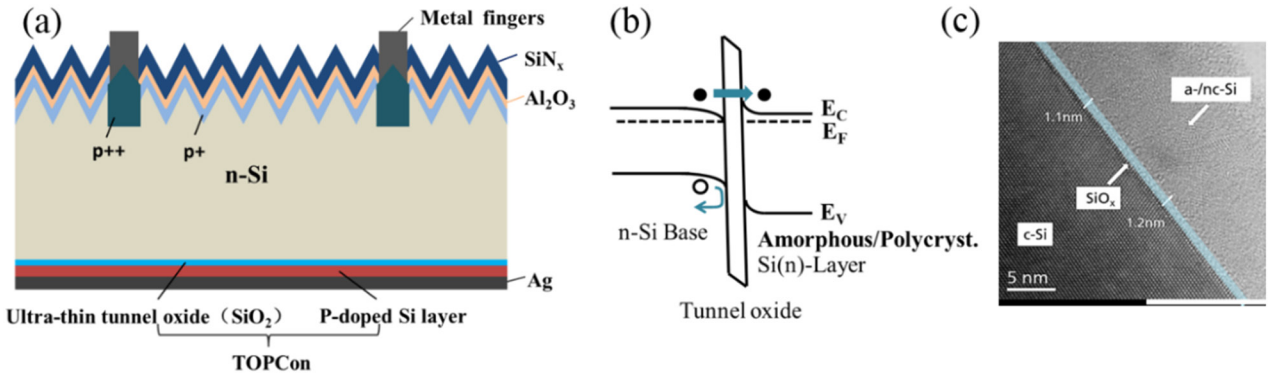

Figure 4. (a) Scheme of the tunnel oxide passivated contact (Fraunhofer TOPCon) cell. (b) The band diagram of the TOPCon cell based on n-type Si wafers. (c) TEM image of the cross section of the TOPCon cell. (c) Reproduced with permission from [55].

layer. Moreover, the symmetric structure prominently reduces the mechanical stress within the wafers. A bifaciality ratio of 79% has been obtained referring to a front efficiency of 20.8% and 16.5% on the rear side.

Some researchers pointed out that the continuous developments of industrial-type PERC cells may lead to cell efficiencies beyond 24% [55]. In the near future, the key improvements of PERC cells include advanced emitter structures such as selective emitters, boron-added Al paste for the rear, wafers with 1 ms lifetime, multi wires instead of busbars and 10 μm narrow fingers with high aspect ratio. The ITRPV 2016 predicts that the market share of the PERC cell structure will increase to 30% by 2020, and this ratio will rise further to 46% in 2026 [56]. As for the bifacial solar cell, the latest ITRPV 2017 predicts a 30% market share in 2027 [25].

2.2. Tunnel oxide passivated contact solar cell

As discussed above, PERC cells have a relatively perfect passivation scheme, but the fabrication process is kind of complicated because the rear contact is restricted to the opening region and the opening process may often cause damage to the surrounding silicon material. In addition, the apertures may prevent the carriers from transporting along the shortest path perpendicular to the contact surface resulting in the carriers crowded at the opening. In 2013, Fraunhofer ISE developed a novel technology, namely the tunnel oxide passivated contact (TOPCon) technology [57–59], which is a good solution to the above problems. An ultrathin layer of SiO_2 with a thickness of 1–2 nm was prepared by wet chemical method on the rear side of the solar cell. Subsequently, a 20 nm phosphorus doped silicon layer was deposited on the SiO_2 layer, and high temperature annealing was applied to transform the silicon layer into doped polysilicon, which combined with the SiO_2 layer to form the TOPCon structure, replacing the fully doped rear surface of the traditional screen-printed Al-BSF solar cell. Finally, physical vapor deposition (PVD) was used to form a full silver rear contact. At the very beginning, a conversion efficiency of 23.0% was obtained. The design of full-rear metal contact sheds the constraint of the local contact opening for the carrier transport path in PERC cell structure, making the current simply and effectively transport along the shortest path of one dimension, and radically suppresses series resistance loss, thereby improving the fill factor (FF). In addition, such TOPCon design not only has high temperature stability, but also greatly simplifies the fabrication process.

In 2015, Fraunhofer ISE announced a 25.1% [60] conversion efficiency ($V_{oc} = 718$ mV, $J_{sc} = 42.1$ mA cm^{-2}, FF = 83.2%) on a 200 μm thick, n-type 1 Ω cm Fz silicon substrate with cell area of 4 cm^2. The rear side of the cell adopted Topcon structure and full-Ag rear contact, and the selective emitter structure with boron diffusion was used on the front side, then ALD Al_2O_3 and PECVD SiN_x were deposited to passivate the surface and reduce the reflection. Figures 4(a) and 6(b) show the scheme and band diagram of the tunnel oxide passivated contact (Fraunhofer TOPCon) cell based on n-type Si wafers, respectively. It was demonstrated that the efficiency potential of TOPCon cell is rather independent of the base resistivity, giving the TOPCon cell an advantage in production environment because a much wider doping range of the starting material can be adopted. This study also showed that about 50% of the recombination takes place at the front side of the cell. Therefore, further optimization of surface passivation of the front emitter and contacts is required to obtain higher efficiency. One and a half years later, they achieved a new world record efficiency of 25.7% ($V_{oc} = 725$ mV, $J_{sc} = 42.5$ mA cm^{-2}, FF = 83.3%) with an absolute gain of 0.6% based on the TOPCon technology for both sides-contacted monocrystalline silicon solar cells [61].

For large-area n-type Si solar cells based on the TOPCon structure, Tao *et al* combined the tunnel oxide layer with the screen-printed front contact on homogeneous boron emitter to provide sufficient surface passivation, and finally obtained a cell efficiency of 21.4% ($V_{oc} = 674$ mV, $J_{sc} = 39.6$ mA cm^{-2}, FF = 80.0%) on 239 cm^2 commercial grade n-type Cz wafers [62]. Detailed study showed that a cell efficiency over 22.5% can be achieved by introducing a selective emitter underneath the metal contact to reduce the recombination at the metal semiconductor front contact. In 2016, a conversion efficiency of 25% was announced on a 3.97 cm^2 passivated rear contact silicon solar cell by ISFH and Gottfried Wilhelm Leibniz Universität Hannover at the 26th International Photovoltaic Science and Engineering Conference (PVSEC) [63]. The main reason for this high efficiency lies in the 'POLO' (polysilicon oxide) contact point consisting of doped polysilicon layer and thin silicon oxide. This POLO layer can

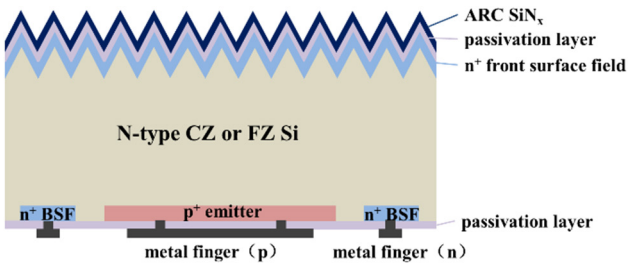

Figure 5. Scheme of an IBC solar cell with n^+ BSF (back surface field), p^+ emitter and contacts located on the rear side of the solar cell in an interdigitated structure.

significantly suppress the surface recombination underneath the metal contact and thus increase the open-circuit voltage up to 723 mV. At the same time, the two poles of POLO layer were placed at the rear side of the cell, reducing both the shading loss of the front side and the parasitic absorption of polysilicon. Recently, simulation studies showed that 23.2% efficiency can be achieved for single sided TOPCon cells on large-area Cz substrates with a resistivity of 10 Ω cm and a bulk lifetime of 3 ms [64].

2.3. IBC solar cell

IBC solar cell is one of the important ways to realize high-efficiency crystalline silicon solar cell, becoming increasingly considered as a promising route for large-scale industrial production, to continue the ongoing trend of increasing commercial efficiency.

Both the emitter and the BSF doping layer with their corresponding metallization grids are located in an interdigitated structure on the back side of the solar cell, as shown in figure 5. The most outstanding feature of the cell structure is the employment of all rear contacts, which completely eliminates optical shading losses on the front side. Therefore, IBC solar cell usually has an increased absorption and short circuit current density. The other advantages are as follows: (1) due to the absence of the front metal fingers, there is no need to consider the contact resistance on the front side, providing more space and potential for the optimization of the front surface passivation performance; (2) since the front metal fingers shading losses are not taken into account, wider fingers could be used to decrease the series resistance of the metal contact on the rear side; (3) the design of all rear contacts makes cell interconnection in modules more simple and beautiful.

In general, the IBC cells are mainly fabricated on n-type silicon substrates with boron-diffused emitters. The pyramid structure and the antireflection layer on the front side improve the light-trapping effect, while the thermal SiO_2 passivation layers at the front and rear surfaces reduce the surface recombination and increase the long wave response, thus improving the open-circuit voltage. The FSF underneath the SiO_2 passivation layers acts as an electrical field that repels the minority carriers at the front surface and thus reduces the front surface recombination. The rear metal electrode formed by screen printing realizes the point contact with the silicon substrate by passing through the contact hole in the SiO_2 passivation layer, which can reduce the contact area between the metal electrode and the silicon wafer and thus further suppress the carrier recombination at the contact interface.

The essential question of IBC solar cell is how to prepare n-regions and p-regions with good quality and interdigitated distribution on the rear surface. In order to avoid the non-uniform diffusion and high temperature damage in traditional liquid boron diffusion process, the complexity of the operation and increasing costs due to multiple lithography, the process can be simplified. A boron-doped diffusion mask layer with interdigitated structure is printed on the rear surface, and the boron in the mask layer diffuses into the n-type substrate to form the p+ region, while the unprinted regions form the n+ region by phosphorus diffusion. But some problems still exist for the screen printing process because of the accuracy of alignment and printing repeatability. Doping via ion implantation is widely used in semiconductor industry. In recent years, ion implantation has been applied to the IBC solar cell because this technology can precisely control the doping concentration to achieve uniform p-region and n-region with controllable junction depth. Furthermore, this doping technique allows for single side doping, which simplifies the fabrication process. However, it requires high annealing temperature for drive-in and activation of the dopants, which is thus a difficult problem in the PV industry [65–69]. In addition, laser doping [70] is another option to replace the traditional thermal diffusion with advantages such as easy control of doping depth and concentration, and pattern-ability of doping area without lithography. The dopant source can be gas, liquid, or solid [71]. Selective doping area, for example, selective emitter could be obtained by laser doping technology without the entire silicon substrate suffering from the high temperature process [72–74]. Along with its applications in laser texturing [75], laser ablation for contact opening [74] and laser-fired contact in solar cells [76, 77], laser technique has a promising prospect in solar cells.

Compared with conventional crystalline silicon cells, the surface recombination of front surface has a greater impact on the performance of IBC solar cell because the front surface is far away from the p-n junction, which is located on the rear side. In order to suppress the front surface recombination, a better surface passivation scheme is required for the front surface. At the same time, high quality base material with long diffusion length is often needed to ensure that photon-generated minority carriers do not recombine before arriving at the back junction.

SunPower Corp. has been in a leading position in the research and development of IBC solar cells, and has achieved an average efficiency of mass production up to 23%. In 2014, they obtained an efficiency of 25% ($V_{oc} = 725.6$ mV, $J_{sc} = 41.53$ mA cm^{-2}, FF = 82.84%) in laboratory by optimizing surface passivation [16]. In October 2016, SunPower announced a high conversion efficiency of 25.2% ($V_{oc} = 737$ mV, $J_{sc} = 41.33$ mA cm^{-2}, FF = 82.7%) by further reducing edge loss, series resistance and the emitter recombination based on its X-Series cell structure on a 130 μm thick, n-type CZ silicon substrate [78], with a total cell area of 153.49 cm^2. This was the first time that large area crystalline silicon solar

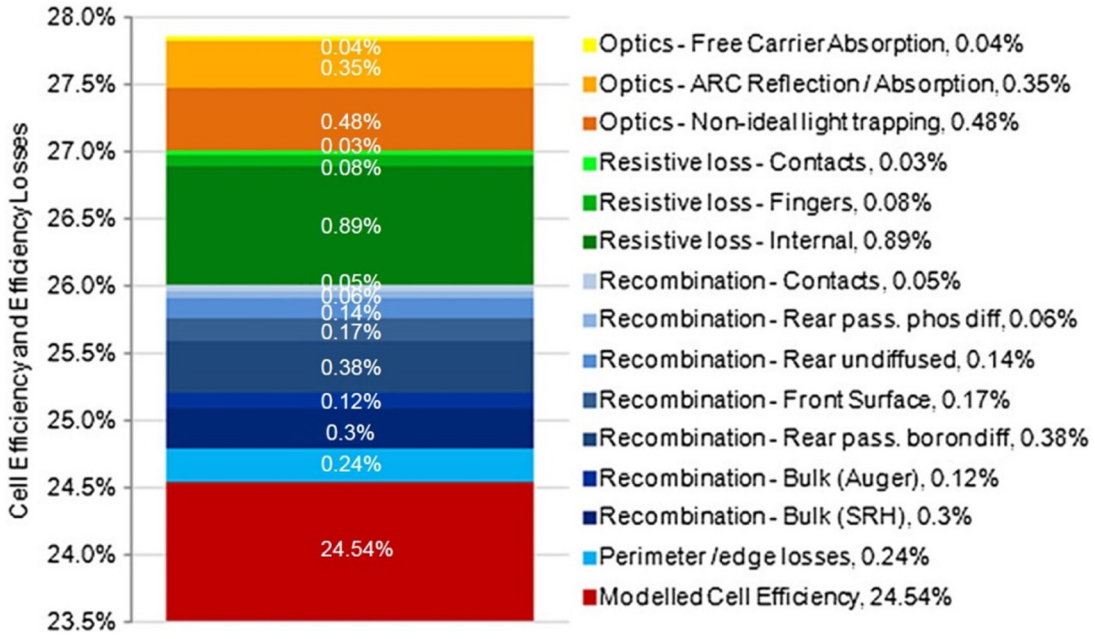

Figure 6. Modelled cell efficiency and detailed breakdown of all losses for the 24.4% efficient IBC cell. Modelling is conducted via Quokka 3D device simulation and optical ray tracing by utilizing the free energy loss analysis method, with modelling inputs based on the measured physical, electronic and optical properties of the cell itself, accompanying test structures or co-processed monitor wafers. [82] John Wiley & Sons. Copyright © 2014 John Wiley & Sons, Ltd.

cells having a conversion efficiency beyond 25%. The first module was composed of 72 IBC cells with median efficiency of approximate 25%, having a final record module efficiency of 24.1%.

Apart from SunPower, Sharp and Panasonic combined silicon heterojunction (SHJ) with IBC technology and achieved a conversion efficiency of up to 25.6% [14, 15] in 2014. IMEC, Fraunhofer ISE and ISFH reported efficiency values of 23.3%, 23% and 23.1% for IBC cells fabricated in research institute labs with small area ($2 \times 2\,\mathrm{cm}^2$), respectively [79–81]. The Australian National University (ANU) cooperating with Trina Solar developed a small area ($4\,\mathrm{cm}^2$) IBC solar cell with an efficiency of 24.4% ($V_{oc} = 703$ mV, $J_{sc} = 41.95$ mA cm^{-2}, FF = 82.7%) [82]. Modelling via Quokka 3D device simulation and free energy loss analysis (FELA) method were used to quantify each of the major loss mechanisms within the 24.4% IBC solar cell. Detailed breakdown of all losses are shown in figure 6. Loss analysis revealed that recombination, resistive and optical losses in total amount to 1.23, 0.87 and 1.00%, respectively, while edge losses is only 0.24%. Therefore, considerable efficiency gains can be achieved by using high-quality base material, improving light trapping via surface treatments, optimizing rear surface passivation, and alleviating edge losses. Additionally, recent studies have shown that the IBC cell performance significantly depends on the pitch size (the period in which the alternating doping repeats) and the emitter fraction (namely the ratio of the emitter size to the pitch size). Higher short-circuit current values are often observed for IBC cells with larger emitter fractions. However, larger emitter coverage often leads to more series resistance loss. Therefore, a balance between higher short-circuit current and more series resistance loss should be considered to obtain the maximal efficiency. In general, the emitter fraction is between 70% and 80% for the typical IBC cell designs. Furthermore, smaller the size of the pitch, shorter the mean transport distance to the base contact of the carriers, thereby reducing resistance and recombination loss. However, this would also result in a higher demand for manufacturing process accuracy.

As a promising route to keep up with the ongoing trend of increasing commercial efficiency for large-scale industrial production, IBC solar cell is also becoming more and more attractive for cell manufacturers. Bosch and Samsung applied ion implantation to large-area IBC cells and achieved 22.1 and 22.4% [65, 82], respectively. Trina Solar used low-cost industrial processing technologies such as tube diffusion and screen printing for IBC cells and achieved 22.9% conversion efficiency ($V_{oc} = 683$ mV, $J_{sc} = 41.6$ mA cm^{-2}, FF = 80.6%) on a 156×156 mm² pseudo-square wafer [83]. By further optimizing rear patterning and metal contact area, a conversion efficiency of 23.5% was realized in 2016. Afterwards, in May 2017 Trina Solar announced a conversion efficiency of 24.13% for large area IBC solar cells using available PERC solar cell production lines, actively promoting the industrialization of high-efficiency IBC solar cells [84]. Aiming at large-scale commercial manufacturing of IBC solar cells, ANU adopted damage-free laser ablation instead of multiple photolithographic patterning steps for wafer patterning and utilized laser doping in place of thermal diffusion to reduce complexity and eliminate high temperature process. Finally, they achieved an efficiency of 23.5% [82]. In 2016, Dahlinger *et al* developed IBC solar cells with a pitch below 500 μm using laser doping including boron and phosphorus doping as well as laser ablation including contact opening and metallization patterning instead of multiple photolithographic steps and achieved an efficiency of 23.24% [74].

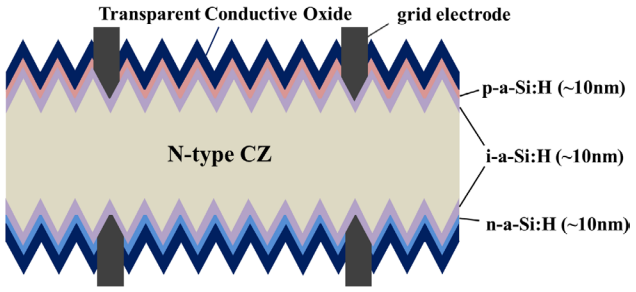

Figure 7. Scheme of a HIT solar cell.

2.4. HIT solar cell

HIT solar cells is a further improved version of silicon heterojunction (SHJ) solar cell. SHJ solar cells consist of the doped hydrogenated amorphous silicon and crystalline silicon substrate, however the efficiency is usually low because of the unpassivated c-Si surfaces. In 1991, Sanyo Co. Ltd (now Panasonic Co. Ltd) inserted a very thin intrinsic a-Si layer between the doped a-Si layer and the c-Si substrate, named HIT (heterojunction with intrinsic thin-layer) solar cell. The HIT solar cells can effectively separate the electron hole pairs due to the higher built-in field compared to the traditional homogeneous crystalline silicon cells. Furthermore, the a-Si:H layer has an excellent passivation effect on crystalline silicon surface to decrease the interface state density and thus reduce the surface recombination. Both of these two characteristics make HIT solar cells have higher open-circuit voltage and higher efficiency.

HIT solar cell has been attracting a growing amount of attention year by year due to the following advantages: (1) structural symmetry: compared to conventional crystalline silicon solar cell, the symmetrical structure reduces the mechanical stress, and therefore the thickness of the cell and the production cost can be reduced greatly. Meanwhile, the bifacial modules consisting of such symmetrical HIT cells can adsorb light from double sides and thus improve the generating capacity; (2) low temperature process: low temperature process (below 200 °C) can not only save energy, but also prevent any degradation of bulk quality that happen with high-temperature cycling process in low-quality silicon materials such as solar grade crystalline Si; (3) high open circuit voltage: both the large band bending between amorphous Si and crystalline Si and the excellent surface passivation of crystalline Si surface by intrinsic amorphous Si result in a high open-circuit voltage and a high conversion efficiency; (4) good stability: n-type silicon wafers are used as the substrate without light-induced degradation. Additionally, a much better temperature coefficient can be obtained for HIT solar cells compared with conventional diffused cells.

A typical scheme of the n-type Si HIT solar cell is shown in figure 7. The n-type CZ Si substrate is first cleaned and textured for double sides. Afterwards, a 5–10 nm intrinsic amorphous Si layer and a 5–10 nm p-type amorphous Si layer are deposited successively on the front side by PECVD method to form the p-n junction. On the rear side, the BSF structure is composed of symmetrical stacking layers namely a 5–10 nm intrinsic amorphous Si layer and a 5–10 nm n-type amorphous

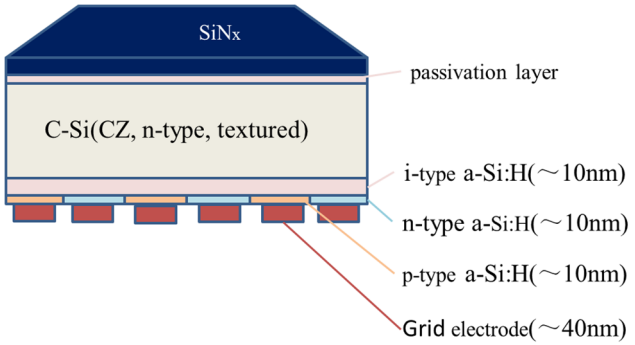

Figure 8. Scheme of a HBC solar cell.

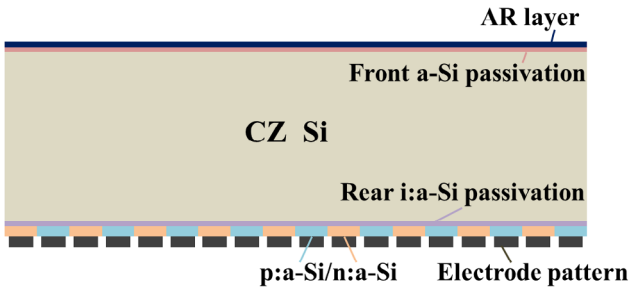

Figure 9. Scheme of the record HBC solar cell.

Si layer. Finally, TCO layers and metal electrodes are synthesized by sputtering and screen-printing methods, respectively, on both surfaces. All processes (including metallization process) are performed at temperatures of below 200 °C.

Up to now, the HIT solar cell has been in development for more than twenty years since an efficiency of 20% was first achieved for HIT solar cells with an aperture area of 1 cm^2 by Sanyo [85]. After that, Sanyo have continuously been devoting to the optimization of HIT solar cells in the following aspects: (1) creating a better hetero-interface by cleaning the c-Si wafer as much as possible and using a low-damage plasma deposition processes for high-quality a-Si:H films [86, 87]; (2) reducing optical loss and electrical loss by optimizing the viscosity and rheology of low temperature silver paste during the screen printing process as well as the grid electrode with larger aspect ratio and lower resistance; (3) reducing optical loss by developing high-quality wide-gap alloys such as a-SiC:H and high-quality TCO with high carrier mobility; (4) reducing the material cost by using thinner wafers [88, 89]. As a result, in February 2013, Panasonic Corporation achieved a conversion efficiency of 24.7% (V_{oc} =750 mV, J_{sc} = 39.5 mA cm^{-2}, FF = 83.2%) for a 98 μm thick and 101.8 cm^2 size cell [90]. Then in 2015, a record efficiency of 25.1% (V_{oc} = 738 mV, J_{sc} = 40.8 mA cm^{-2}, FF = 83.5%) was achieved by Kaneka for HIT solar cells based on 160 μm-thick, 6-inch n-type industrial Cz Si wafers [91].

Since the core patent of HIT solar cells owned by Sanyo Co. Ltd expired in 2010, more and more researchers have been devoted to research and development of such cell structure. Silevo used a tunneling oxidation passivation layer to fabricate large-area (239 cm^2) HIT solar cells and achieved a conversion efficiency of 23.1% (V_{oc} = 739 mV, J_{sc} = 39.9 mA cm^{-2}, FF = 80.5%). In 2013, INES in France and Kaneka

Table 1. High efficiency silicon-based solar cell.

Research institute	Cell structure	Wafer type	Cell area (cm^2)	V_{oc} (mV)	J_{sc} (mA $\cdot$ cm^{-2})	FF (%)	Effic. (%)	Ref.
LERRI	PERC	—	—	—	—	—	23.26	[49]
Fraunhofer ISE	TOPCon	n-type Fz	4	725	42.5	83.3	25.7	[61]
SunPower	IBC	n-type Cz	153.49	737	41.33	82.7	25.2	[78]
Kaneka	HJ	n-type Cz	151.9	738	40.8	83.5	25.1	[91]
Kaneka	HBC	n-type Cz	179.7	740	42.5	84.6	26.6	[18]

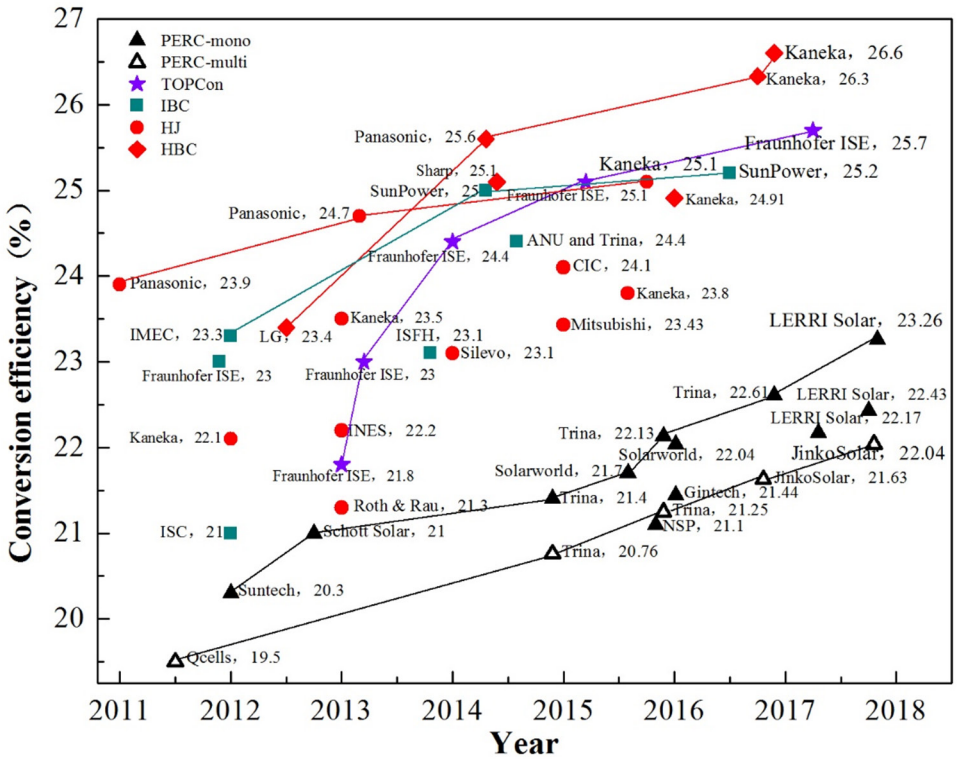

Figure 10. The evolution of the energy conversion efficiencies of crystalline silicon solar cells with the years (2011–2017) for each technology. Advanced manufacturer as Kaneka, Fraunhofer ISE and SunPower *et al* are included as well as some else institutions. (ANU-Australian National University, ISFH-Institute for Solar Energy Research in Hamelin, IMEC-Interuniversity Microelectronics Center, ISC-International Solar Energy Research Center-Konstanz, CIC-Choshu Industry Corporation) The lines are guides to the eye.

in Japan utilized electroplated copper electrodes to reduce the consumption of noble metal Ag and obtained efficiencies of 22.2% ($V_{oc} = 730$ mV, $J_{sc} = 38.7$ mA cm^{-2}, FF = 78.5%) on the 104 cm^2 substrate and 23.5% ($V_{oc} = 737$ mV, $J_{sc} = 39.97$ mA cm^{-2}, FF = 79.8%) on the 239 cm^2 substrate, respectively [92]. CSEM in Switzerland and Meyer Burger, a supplier of large-scale photovoltaic equipment achieved a high conversion efficiency of 22.4–22.7% by establishing an experimental platform of copper electroplated metal electrode and testing the inkjet printing metal electrode to realize low-cost metallization process.

Up to now, enterprises that have achieved industrialization in HIT solar cells include Panasonic, CIC, Kaneka, Solar City and Sunpreme, etc [93]. The lab-efficiency of HIT solar cells in ENN and Shanghai institute of microsystem and information technology reached 22.6% and 23.1%, respectively. In addition, Shanghai institute of microsystem and information technology also obtained a pilot efficiency beyond 22% and has been pushing for large-scale industrialization. It has been acknowledged that HIT solar cells would have a large technical potential to reduce the cost and compete with conventional Si solar cells by further reducing the thickness of Si wafer, optimizing the metal electrode, improving the TCO materials and amorphous silicon thin film, as well as achieving localization of the key equipment and raw materials.

2.5. HBC solar cell

Applying the interdigitated back contact idea to the heterojunction structure, the so-called HBC solar cell is produced. The former has a high short-circuit current density J_{sc} since there is no shading effect for such interdigitated back contact cells, while the latter brings a high V_{oc} because of the high-quality passivation for such heterojunction solar cells. The coalescence of two advanced technologies has been an important and reliable way to improve the efficiency of crystalline silicon cells nowadays. Figure 8 outlines the schematic structure of HBC solar cell.

A passivation layer with good transparency and low surface recombination velocity is deposited on the textured front surface of the c-Si wafer. Then, silicon nitride is deposited to act as an antireflective layer. Afterwards, two stacking layers namely i-a-Si:H/p-a-Si:H and i-a-Si:H/n-a-Si:H are deposited on the rear surface with interdigitated distribution. Finally, grid electrodes are produced on both the n- and p-type a-Si:H layers by electroplating process. The rear grid electrodes can be wide enough to optimize the electrical performance so that the fill factor can be improved greatly.

A HBC solar cell was first proposed by Sharp, who reported a conversion efficiency of 25.1% ($V_{oc} = 736$ mV, $J_{sc} = 41.7$ mA cm^{-2}, FF = 82.0%) in 2014 [15]. And almost at the same time, Panasonic achieved a higher conversion efficiency of 25.6% ($V_{oc} = 740$ mV, $J_{sc} = 41.8$ mA cm^{-2}, FF = 82.7%), with a designed area of 143.7 cm^2, breaking the efficiency record of crystalline Si based solar cells at that time [14].

In mid-September 2016, Kaneka Corporation announced a conversion efficiency of 26.3% ($V_{oc} = 744$ mV, $J_{sc} = 42.3$ mA cm^{-2}, FF = 83.8%) for HBC solar cells with a 180.4 cm^2 designated area [94], and figure 9 outlines the schematic structure of the record HBC solar cell. The cell was fabricated utilizing an industrially applicable capacitively coupled RF PECVD deposition tool to form a-Si layer on a standard n-type c-Si wafer with a size of 239 cm^2, a thickness of about 165 μm, and a resistivity of ~3 Ω cm. The front surface was textured by anisotropic etching to minimize the light reflection, while the rear interdigitated pattern was optimized to minimize the series resistance and the recombination. Consequently, a high conversion efficiency of 26.3% was achieved, which is an improvement of 2.7% relative to the previous record efficiency of 25.6%. Before long, they achieved the highest conversion efficiency of 26.6% ($V_{oc} = 740$ mV, $J_{sc} = 42.5$ mA cm^{-2}, FF = 84.6%) for HBC solar cells based on n-type c-Si wafer with a size of 243 cm^2, a thickness of 200 μm, and a resistivity of ~7 Ω cm [18]. This record conversion efficiency of 26.6%, 0.3% absolute improvement can be mainly attributed to the increase of FF from 83.8% to 84.6% due to the 30% reduction of series resistance. The efficiency records of the above high efficiency crystalline silicon solar cells are shown in table 1 and the reported efficiency of crystalline silicon solar cells with the years (2011–2017) for each technology is shown in figure 10.

3. Summary and outlook

Looking back to the development history of high-efficiency crystalline silicon solar cells in recent decades, the increase in efficiency are mainly due to the following technical developments: photo-lithographically defined metallization, shallow junction, surface texturing, replacement of full Al-BSF, improvements in front and rear passivation, antireflection coatings as well as selective emitter, and elimination of optical shading losses. Among them, surface passivation is the most important technology, which can effectively suppress the recombination of photo-generated carriers especially for future thinner substrates. Encouragingly, several interesting and promising device concepts have emerged as a result of the extensive research and development on high-efficiency Si solar cells. In recent years, the record efficiency is refreshed over and over again. It is well known that PERC solar cells are the most promising for industrialization and commercialization due to their compatibilities with the present industrial p-type Si wafer solar cell processes and less use of elaborate technologies including metallization and lithography. It is estimated that PERC solar cells will continue to compete with the traditional crystalline Si solar cell market in the next few years.

So far, the representative record efficiency values for HBC, TOPCon and IBC solar cells are 26.6%, 25.7% and 25.2%, respectively. All these solar cells are fabricated on n-type substrates, which do not suffer from light-induced degradation and show high tolerance to metal impurities, resulting in higher bulk-carrier lifetime compared with p-type wafers. The continuous success of HBC and TOPCon confirmed the future technical routine for high-efficiency crystalline silicon solar cells, which include hetero-junction, back contact and passivated contact technologies.

In addition, the technology optimization of metallization paste is also a hot research in the PV industry because it is the key auxiliary material for the production of crystalline silicon solar cell and accounts for about 50–60% of the non-silicon cost. As this technology advances, the consumption of paste in single cell continues to decrease, making it another driving force to reduce cell costs in addition to the reduction of silicon wafer costs. By reducing the manufacturing costs and improving the performance of the cell and module, simplifying the processes to reduce the cost of photovoltaic systems so as to ensure the competitiveness of photovoltaic generation. Continuously decreasing cost of photovoltaic energy, especially produced by Si solar cells is likely to underpin utilization of renewable energy in diverse commercially important areas such as industrial chemistry and catalysis, agribusiness, general manufacturing and other economy sectors.

Acknowledgments

This work was partially supported by the National Natural Science Foundation under Grant 61404061, the Natural Science Foundation of Jiangsu Province, China under Grant BK20140168, the Joint Innovation Project of Jiangsu Province under Grant BY2014023-19, the Fundamental Research Funds for the Central Universities of China under Grant JUSRP51726B, the 111 Project under Grant B12018.

ORCID iDs

Shaoqing Xiao https://orcid.org/0000-0002-0564-5532

References

[1] Chapin D M, Fuller C S and Pearson G L 1954 A new silicon p-n junction photocell for converting solar radiation into electrical power *J. Appl. Phys.* **25** 676–7

[2] Bohua W 2016 Development status and prospect of China PV industry *Proc. 12th China SOG Silicon and PV Power Conf. (Jiaxing, China)*

[3] Zhuang Y F, Zhong S H, Huang Z G and Shen W Z 2016 Versatile strategies for improving the performance of diamond wire sawn mc-Si solar cells *Sol. Energy Mater. Sol. Cells* **153** 18–24

[4] Zhang Y, Tao J, Chen Y, Xiong Z, Zhong M, Feng Z and Chu J 2016 A large-volume manufacturing of multi-crystalline silicon solar cells with 18.8% efficiency incorporating practical advanced technologies *RSC Adv.* **6** 58046–54

[5] Cao F, Chen K, Zhang J, Ye X, Li J, Zou S and Su X 2015 Next-generation multi-crystalline silicon solar cells: diamond-wire sawing, nano-texture and high efficiency *Sol. Energy Mater. Sol. Cells* **141** 132–8

[6] Ye X, Zou S, Chen K, Li J, Huang J, Cao F and Su X 2014 18.45%-efficient multi-crystalline silicon solar cells with novel nanoscale pseudo-pyramid texture *Adv. Funct. Mater.* **24** 6708–16

[7] Dullweber T and Schmidt J 2016 Industrial silicon solar cells applying the passivated emitter and rear cell (PERC) concept-a review *IEEE J. Photovolt.* **6** 1366–81

[8] Dullweber T, Hannebauer H and Baumann U 2014 Fine-line printed 5 busbar PERC solar cells with conversion efficiencies beyond 21% *Proc. 29th European Photovoltaic Solar Energy Conf. (EUPVSEC-29) (Amsterdam, Netherlands)* pp 621–6

[9] Jun L 2016 Mono-crystal technology integration of whole PV industry chain *Proc. 12th China SOG Silicon and PV Power Conf. (Jiaxing, China)*

[10] Weiming L 2016 Research and industrialization of PERC solar cell *Proc. 12th China SOG Silicon and PV Power Conf. (Jiaxing, China)*

[11] Fengbing S 2015 Design thinking and solution for high quality and high performance crystalline silicon products-explorations with certain issues *Proc. 11th China SOG Silicon and PV Power Conf. (Hangzhou, China)*

[12] Zhou Jie 2015 High power mono-crystal PERC module researches and industrialization *Proc. 11th China SOG Silicon and PV Power Conf. (Hangzhou, China)*

[13] Xinwei N 2015 Independent integration for mass production of poly-crystal PERC solar cell technology *Proc. 11th China SOG Silicon and PV Power Conf. (Hangzhou, China)*

[14] Masuko K, Shigematsu M, Hashiguchi T, Fujishima D, Kai M, Yoshimura N and Yamanishi T 2014 Achievement of more than 25% conversion efficiency with crystalline silicon heterojunction solar cell *IEEE J. Photovolt.* **4** 1433–5

[15] Nakamura J, Asano N, Hieda T, Okamoto C, Katayama H and Nakamura K 2014 Development of heterojunction back contact Si solar cells *IEEE J. Photovolt.* **4** 1491–5

[16] Smith D D, Cousins P, Westerberg S, De Jesus-Tabajonda R, Aniero G and Shen Y C 2014 Toward the practical limits of silicon solar cells *IEEE J. Photovolt.* **4** 1465–9

[17] Green M A 2009 The path to 25% silicon solar cell efficiency: history of silicon cell evolution *Prog. Photovolt. Res. Appl.* **17** 183–9

[18] Yoshikawa K, Yoshida W, Irie T, Kawasaki H, Konishi K, Ishibashi H and Yamamoto K 2017 Exceeding conversion efficiency of 26% by heterojunction interdigitated back contact solar cell with thin film Si technology *Sol. Energy Mater. Sol. Cells* **173** 37–42

[19] Nelson J 2003 The physics of solar cells *Imperial Coll. Press* **57** 384

[20] Meng T 2014 Physics of solar cells *Terawatt Solar Photovoltaics* (London: Springer) pp 21–45

[21] Shen W Z and Li Z P 2014 *Physics and Devices of Silicon Heterojunction Solar Cells* (Beijing: Science Press) pp 2–6

[22] Nat R and Würfel E P 2011 *Physics of Solar Cells: From Principles to New Concepts* (Darmstadt: Wiley) pp 11–21

[23] Green M A, Zhao J, Wang A, Reece P J and Gal M 2001 Efficient silicon light-emitting diodes *Nature* **412** 805–8

[24] Battaglia C, Cuevas A and De Wolf S 2016 High-efficiency crystalline silicon solar cells: status and perspectives *Energy Environ. Sci.* **9** 1552–76

[25] Crystalline Silicon PV Technology and Manufacturing (CTM) Group 2017 International technology roadmap for photovoltaic (ITRPV.net) Results 2016 8th edn (www.itrpv.net/Reports/Downloads/2017/)

[26] Xiao S Q and Xu S 2014 High-efficiency silicon solar cells-materials and devices physics *Crit. Rev. Solid State* **39** 277–317

[27] Xiao S Q, Xu S and Ostrikov K 2014 Low-temperature plasma processing for Si photovoltaics *Mater. Sci. Eng.* R **78** 1–29

[28] Green M A, Blakers A W and Kurianski J 1984 Ultimate performance silicon solar cells *NERDDP Project* 81/1264

[29] Green M A, Blakers A W, Zhao J, Milne A M, Wang A and Dai X 1990 Characterization of 23-percent efficient silicon solar cells *IEEE Trans. Electron Dev.* **37** 331–6

[30] Dullweber T, Siebert M, Veith B, Kranz C, Schmidt J and Brendel R 2012 High-efficiency industrial-type PERC solar cells applying ICP AlOx as rear passivation layer *Proc. 27th European Photovoltaic Solar Energy Conf. (EUPVSEC-27) (Frankfurt, Germany)* pp 672–5

[31] Dingemans G, Seguin R, Engelhart P, Sanden M C M V D and Kessels W M M 2010 Silicon surface passivation by ultrathin Al_2O_3 films synthesized by thermal and plasma atomic layer deposition *Phys. Status Solidi: Rap. Res. Lett* **4** 10–12

[32] George S M 2010 Atomic layer deposition: an overview *Chem. Rev.* **110** 111–31

[33] Knapas K and Ritala M 2013 *In situ* studies on reaction mechanisms in atomic layer deposition *Crit. Rev. Solid State* **38** 167–202

[34] Ponraj J S, Attolini G and Bosi M 2013 Review on atomic layer deposition and applications of oxide thin films *Crit. Rev. Solid State* **38** 203–33

[35] Xu S, Levchenko I, Huang S Y and Ostrikov K 2009 Self-organized vertically aligned single-crystal silicon nanostructures with controlled shape and aspect ratio by reactive plasma etching *Appl. Phys. Lett.* **95** 111505

[36] Levchenko I, Ostrikov K, Keidar M and Xu S 2005 Microscopic ion fluxes in plasma-aided nanofabrication of ordered carbon nanotip structures *J. Appl. Phys.* **98** 129

[37] Chryssou C E and Pitt C W 1997 Al_2O_3 thin films by plasma-enhanced chemical vapour deposition using trimethyl-amine alane (TMAA) as the Al precursor *Appl. Phys.* A **65** 469–75

[38] Saint-Cast P, Kania D, Hofmann M, Benick J, Rentsch J and Preu R 2009 Very low surface recombination velocity on p-type c-Si by high-rate plasma-deposited aluminum oxide *Appl. Phys. Lett.* **95** 151502

[39] Miyajima S, Irikawa J, Yamada A and Konagai M 2009 High quality aluminum oxide passivation layer for crystalline silicon solar cells deposited by parallel-plate plasma-enhanced chemical vapor deposition *Appl. Phys. Express* **3** 012301

[40] Zhou H P, Xu L X, Xu S, Huang S Y, Wei D Y, Xiao S Q and Xu M 2010 On conductivity type conversion of p-type silicon exposed to a low-frequency inductively coupled plasma of Ar + H_2 *J. Phys. D: Appl. Phys.* **43** 505402

[41] Xiao S Q and Xu S 2011 Plasma-aided fabrication in Si-based photovoltaic applications: an overview *J. Phys. D: Appl. Phys.* **44** 174033

[42] Xiao S Q, Xu S, Zhou H P, Wei D Y, Huang S Y, Xu L X and Khan S 2012 Amorphous/crystalline silicon heterojunction solar cells via remote inductively coupled plasma processing *Appl. Phys. Lett.* **100** 233902

[43] Zhou H P, Wei D Y, Xu S, Xiao S Q, Xu L X, Huang S Y and Xu M 2012 Si surface passivation by SiO_x: H films deposited by a low-frequency ICP for solar cell applications *J. Phys. D: Appl. Phys.* **45** 395401

[44] Hannebauer H, Dullweber T, Baumann U, Falcon T and Brendel R 2015 21.2%-efficient fineline-printed PERC solar cell with 5 busbar front grid *Phys. Status Solidi: Rap. Res. Lett.* **8** 675–9

[45] Dullweber T, Hannebauer H, Dorn S, Schimanke S, Merkle A and Hampe C 2016 Emitter saturation current densities of 22 fA cm^{-2} applied to industrial PERC solar cells approaching 22% conversion efficiency *Prog. Photovolt. Res. Appl.* **25** 509–14

[46] Ye F, Deng W, Guo W, Liu R, Chen D and Chen Y 2016 22.13% efficient industrial p-type mono PERC solar cell *Proc. 43rd IEEE Photovoltaic Specialists Conf. (PVSC) (Portland, OR)* p 3360

[47] Dullweber T, Hannebauer H, Dorn S, Schimanke S, Merkle A, Hampe C and Brendel R 2017 Emitter saturation current densities of 22fA/cm^2 applied to industrial PERC solar cells approaching 22% conversion efficiency *Prog. Photovol. Res. Appl.* **25** 509–14

[48] Deng W, Ye F, Liu R, Li Y, Chen H and Xiong Z 2017 22.61% Efficient fully screen printed PERC solar cell *Proc. 44th IEEE Photovoltaic Specialists Conf. (PVSC) (Washington, DC)*

[49] LONGi Solar 2017 www.longi-solar.com/index.php?m=content&c=index&a=show&catid=98&id=19

[50] Deng W, Ye F, Xiong Z, Chen D, Guo W, Chen Y and Verlinden P J 2016 Development of high-efficiency industrial p-type multi-crystalline PERC solar cells with efficiency greater than 21% *Energy Proc.* **92** 721–9

[51] Zheng P, Xu J, Sun H, Zhang F, Guo Y, Pan H and Zhang X 2017 21.63% industrial screen-printed multicrystalline Si solar cell *Phys. Status Solidi: Rap. Res. Lett.* **11** 1600453

[52] JinkoSolar 2017 www.jinkosolar.com/press_detail_1381.html?lan=cn

[53] Kranz C, Wolpensinger B, Brendel R and Dullweber T 2016 Analysis of local aluminum rear contacts of bifacial PERC + solar cells *IEEE J. Photovolt.* **6** 830–6

[54] Dullweber T, Kranz C, Peibst R, Baumann U, Hannebauer H, Fülle A and Fischer G 2016 PERC + : industrial PERC solar cells with rear Al grid enabling bifaciality and reduced Al paste consumption *Prog. Photovolt. Res. Appl.* **24** 1487–98

[55] Min B, Wagner H, Müller M, Neuhaus H, Brendel R and Altermatt P P 2015 Incremental efficiency improvements of mass-produced PERC cells up to 24% predicted solely with continuous development of existing technologies and wafer materials *Proc. 30th European Photovoltaic Solar Energy Conf. and Exhibition (EUPVSEC-30) (Hamburg, Germany)* pp 473–6

[56] Crystalline Silicon PV Technology and Manufacturing (CTM) Group 2016 International technology roadmap for photovoltaic (ITRPV.net) Results 2015 7th edn (www.itrpv.net/Reports/Downloads/2016/)

[57] Feldmann F, Bivour M, Reichel C, Hermle M and Glunz S W 2014 Passivated rear contacts for high-efficiency n-type Si solar cells providing high interface passivation quality and excellent transport characteristics *Sol. Energy Mater. Sol. Cells* **120** 270–4

[58] Feldmann F, Bivour M, Reichel C, Steinkemper H, Hermle M and Glunz S W 2014 Tunnel oxide passivated contacts as an alternative to partial rear contacts *Sol. Energy Mater. Sol. Cells* **131** 46–50

[59] Moldovan A, Feldmann F, Zimmer M, Rentsch J, Benick J and Hermle M 2015 Tunnel oxide passivated carrier-selective contacts based on ultra-thin SiO_2 layers *Sol. Energy Mater. Sol. Cells* **142** 123–7

[60] Glunz S W, Feldmann F, Richter A, Bivour M, Reichel C, Steinkemper H and Hermle M 2015 The irresistible charm of a simple current flow pattern-25% with a solar cell featuring a full-area back contact *Proc. 31st European Photovoltaic Solar Energy Conf. and Exhibition (EUPVSEC-31) (Hamburg, Germany)*

[61] Chen C W, Hermle M, Benick J, Tao Y G, Ok Y W, Upadhyaya A, Tam A M and Rohatgi A 2017 Modeling the potential of screen printed front junction CZ silicon solar cell with tunnel oxide passivated back contact *Prog. Photovol. Res. Appl.* **25** 49–57

[62] Tao Y, Upadhyaya V, Huang Y Y, Chen C W, Jones K and Rohatgi A 2016 Carrier selective tunnel oxide passivated contact enabling 21.4% efficient large-area N-type silicon solar cells *Proc. 43rd IEEE Photovoltaic Specialists Conf. (PVSC) (Portland, OR)*

[63] ISFH 2016 Passivated contacts silicon solar cells achieved 25% conversion efficiency *Proc. 26th European Photovoltaic Solar Energy Conf. and Exhibition (EUPVSEC-26) (Singapore)*

[64] Chen C W, Hermle M, Benick J, Tao Y, Ok Y W, Upadhyaya A and Rohatgi A 2017 Modeling the potential of screen printed front junction CZ silicon solar cell with tunnel oxide passivated back contact *Prog. Photovolt. Res. Appl.* **25** 49–57

[65] Ingenito A, Isabella O and Zeman M 2016 Simplified process for high efficiency, self-aligned IBC c-Si solar cells combining ion implantation and epitaxial growth: design and fabrication *Sol. Energy Mater. Sol. Cells* **157** 354–65

[66] Yang G, Ingenito A, Isabella O and Zeman M 2016 IBC c-Si solar cells based on ion-implanted poly-silicon passivating contacts *Sol. Energy Mater. Sol. Cells* **158** 84–90

[67] DubÉ C E, Tsefrekas B, Buzby D, Tavares R, Zhang W and Gupta A 2011 High efficiency selective emitter cells using patterned ion implantation *Energy Proc.* **8** 706–11

[68] Feldmann F, Müller R, Reichel C and Hermle M 2015 Ion implantation into amorphous Si layers to form carrier-selective contacts for Si solar cells *Phys. Status Solidi: Rap. Res. Lett.* **8** 767–70

[69] Kang M G, Lee J H, Boo H, Tark S J, Hwang H C and Hwang W J 2012 Effects of annealing on ion-implanted Si for interdigitated back contact solar cell *Curr. Appl. Phys.* **12** 1615–8

[70] Li T, Zhou C L, Zhao L, Li H L, Diao H W, Liu Z G and Wang W J 2011 Research progress of laser doping in preparation of crystalline silicon solar cells *Trans. China Electrotech. Soc.* **26** 141–7

[71] Gall S, Paviet-Salomon B, Lerat J and Emeraud T 2012 Laser doping strategies using SiN:P and SiN:B dielectric layers for profile engineering in high efficiency solar cell *Energy Proc.* **27** 449–54

[72] Gall S, Manuel S and Lerat J F 2013 Boron laser doping through high quality Al_2O_3 passivation layer for localized B-BSF PERL solar cells *Energy Proc.* **38** 270–7

[73] Jäger U, Suwito D, Benick J, Janz S and Preu R 2011 A laser based process for the formation of a local back surface field for n-type silicon solar cells *Thin Solid Films* **519** 3827–30

[74] Dahlinger M, Carstens K, Hoffmann E, Zapf-Gottwick R and Werner J H 2017 23.2% laser processed back contact solar cell: fabrication, characterization and modeling *Prog. Photovolt. Res. Appl.* **25** 192–200

[75] Abbott M and Cotter J 2006 Optical and electrical properties of laser texturing for high-efficiency solar cells *Prog. Photovolt. Res. Appl.* **14** 225–35

[76] Graf M, Nekarda J, Eberlein D, Woehrle N, Preu R, Böhme R and Grosse T 2014 Progress in laser-based foil metallization for industrial perc solar cells *Proc. 29th European Photovoltaic Solar Energy Conf. and Exhibition (EUPVSEC-29) (Amsterdam, The Netherlands)* pp 532–5

[77] Schneiderlöchner E, Preu R, Lüdemann R and Glunz S W 2010 Laser-fired rear contacts for crystalline silicon solar cells *Prog. Photovolt. Res. Appl.* **10** 29–34

[78] Smith D D, Reich G, Baldrias M, Reich M, Boitnott N and Bunea G 2016 Silicon solar cells with total area efficiency above 25% *Proc. 43rd IEEE Photovoltaic Specialists Conf. (PVSC) (Portland, OR)*

[79] Aleman M, Das J, Janssens T, Pawlak B, Posthuma N, Robbelein J and Yoshikawa K 2012 Development and integration of a high efficiency baseline leading to 23% IBC cells *Energy Proc.* **27** 638–45

[80] Reichel C, Granek F, Hermle M and Glunz S W 2013 Back-contacted back-junction n-type silicon solar cells featuring an insulating thin film for decoupling charge carrier collection and metallization geometry *Prog. Photovolt. Res. Appl.* **21** 1063–76

[81] Peibst R, Harder N P, Merkle A, Neubert T, Kirstein S, Schmidt J and Brendel R 2013 High-efficiency RISE IBC solar cells: influence of rear side passivation on pn junction meander recombination *Proc. 28th European Photovoltaic Solar Energy Conf. and Exhibition (EUPVSEC-28) (Paris, France)*

[82] Franklin E, Fong K, McIntosh K, Fell A, Blakers A, Kho T and Wang E C 2016 Design, fabrication and characterisation of a 24.4% efficient interdigitated back contact solar cell *Prog. Photovolt. Res. Appl.* **24** 411–27

[83] Zhang X, Yang Y, Liu W, Zhang K, Chen Y, Li Z and Verlinden P J 2014 Development of high efficiency interdigitated back contact silicon solar cells and modules with industrial processing technologies *Proc. 6th IEEE World Conf. on Photovoltaic Energy Conversion (WCPEC-6) (Kyoto, Japan)*

[84] Franklin E, Fong K, McIntosh K, Fell A, Blakers A, Kho T, Walter D, Wang D, Zin N and Stocks M 2016 Design, fabrication and characterization of a 24.4% efficient interdigitated back contact solar cell *Prog. Photovol. Res. Appl.* **24** 411–27

[85] Sawada T, Terada N, Tsuge S, Baba T, Takahama T, Wakisaka K and Nakano S 1994 High-efficiency a-Si/c-Si heterojunction solar cell *Proc. 1st IEEE World Conf. on Photovoltaic Energy Conversion (WCPEC-1) (Waikoloa, HI)*

[86] Taguchi M, Kawamoto K, Tsuge S, Baba T, Sakata H, Morizane M and Oota O 2000 HIT™ cells-high-efficiency crystalline Si cells with novel structure *Prog. Photovolt.* **8** 503–13

[87] Taguchi M, Terakawa A, Maruyama E and Tanaka M 2005 Obtaining a higher V_{oc} in HIT cells *Prog. Photovolt. Res. Appl.* **13** 481–8

[88] Taguchi M, Tsunomura Y, Inoue H, Taira S, Nakashima T, Baba T and Maruyama E 2009 High-efficiency HIT solar cell on thin ($<$100 μm) silicon wafer *Proc. 24th European Photovoltaic Solar Energy Conf. and Exhibition (EUPVSEC-24) (Hamburg, Germany)*

[89] Kinoshita T, Fujishima D, Yano A, Ogane A, Tohoda S, Matsuyama K and Taguchi M 2011 The approaches for high efficiency HIT solar cell with very thin ($<$100 μm) silicon wafer over 23% *Proc. 26th European Photovoltaic Solar Energy Conf. (EUPVSEC-26) (Hamburg, Germany)*

[90] Taguchi M, Yano A, Tohoda S, Matsuyama K, Nakamura Y, Nishiwaki T and Maruyama E 2014 24.7% record efficiency HIT solar cell on thin silicon wafer *IEEE J. Photovolt.* **4** 96–9

[91] Adachi D, Hernández J L and Yamamoto K 2015 Impact of carrier recombination on fill factor for large area heterojunction crystalline silicon solar cell with 25.1% efficiency *Appl. Phys. Lett.* **107** 233506

[92] Okamoto S 2013 Technology trends of high efficiency crystalline silicon solar cells *Proc. 6th Int. Photovoltaic Power Generation Expo (PV EXPO-6) (Tokyo, Japan)*

[93] Zhengxin L 2016 Silicon heterojunction solar cell technologies and its researches *Proc. 12th China SoG Silicon and PV Power Conf. (Jiaxing, China)*

[94] Yoshikawa K, Kawasaki H, Yoshida W, Irie T, Konishi K, Nakano K and Yamamoto K 2017 Silicon heterojunction solar cell with interdigitated back contacts for a photoconversion efficiency over 26% *Nat. Energy* **2** 17032